

## Impurity Ion Diagnostics in the GAMMA 10 Tandem Mirror

YOSHIKAWA Masayuki\*, OKAMOTO Yuuji, KAWAMORI Eiichiro, ITO Takahiro, WATABE Chikara,  
WATANABE Yoshihiko, IKEDA Katsunori<sup>1</sup>, YAMAGUCHI Naohiro<sup>2</sup>,  
TAMANO Teruo and YATSU Kiyoshi

*Plasma Research Center, University of Tsukuba, Tsukuba, Ibaraki 305-8577, Japan*

<sup>1</sup>*National Institute for Fusion Science, Toki, Gifu 509-5952, Japan*

<sup>2</sup>*Toyota Technological Institute, Tempaku, Nagoya 468-8511, Japan*

(Received: 18 January 2000 / Accepted: 18 April 2000)

### Abstract

We constructed some spectroscopic measurement systems that cover the wavelength range from soft X-ray (SX) to visible lights. We have observed the absolute impurity line intensities, Doppler line broadenings, Doppler shifts by ultraviolet and visible spectrograph and time dependent radial profiles of the impurity lines by the vacuum ultraviolet (VUV) and the SX spectrographs. We determined the radiation loss in the wavelength range from visible to VUV and carbon ion density. These spectroscopic systems could be powerful tools to diagnose the GAMMA 10 plasma in a long pulse operation.

### Keywords:

spectroscopy, UV/V spectrograph, VUV spectrograph, SX spectrograph, GAMMA 10 tandem mirror

### 1. Introduction

Impurity lines and continuum radiation in the wavelength range from visible light to soft X-ray (SX) are emitted from fusion plasmas. These emissions provide us information about radiation power losses, ion density profiles which directly relate to the impurity transport in magnetically confined plasmas and phenomena related to potential formation in the radial direction. We prepared two 2-dimensional ultraviolet and visible (UV/V) spectrograph systems (2000–5000 Å) [1-3], time- and space-resolving vacuum ultraviolet (VUV) (150–1050 Å) [4-7] and SX (20–350 Å) spectrographs [7-9] for impurity diagnostics. These spectroscopic measurement systems can provide simultaneous spectral, temporal and spatial resolution of the plasma radiation. Spectroscopic data taken by these diagnostic systems would be important for long pulse operation of the fusion plasma research.

We have measured the absolute intensities of emitted spectral lines of radial distribution in the

wavelength range from SX to visible lights. In order to obtain impurity ion temperatures, we used the UV/V spectrograph and measure Doppler broadenings of the impurity spectral lines. Radial electrostatic potential profiles have been obtained by measuring Doppler shifts of variously charged impurity ions. In order to measure time dependent impurity ion profiles in the radial direction, the VUV and the SX spectrographs were used. Impurity ion densities have been estimated by using a collisional radiative model (CR-model) calculation code which is provided by T. Kato [10]. We obtained radiation loss in the wavelength range from visible to VUV and the carbon ion density by using these spectroscopic measurements.

### 2. Spectroscopic Diagnostic Systems

The two space-resolving UV/V spectrograph systems view the plasma column vertically. Figure 1 shows the schematic of the UV/V spectrograph. The

*Corresponding author's e-mail: yosikawa@prc.tsukuba.ac.jp*

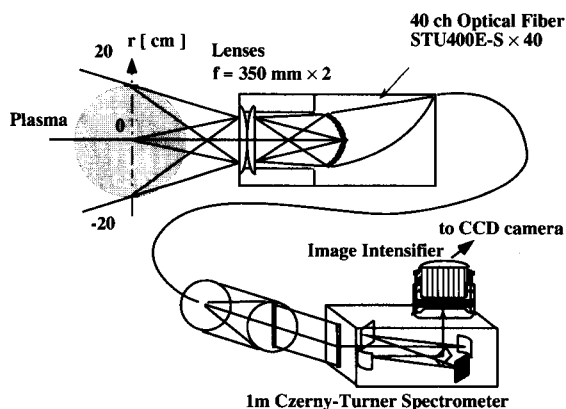


Fig. 1 Schematic of UV/V spectrograph system.

UV/V light from the plasma is collected by a quartz lens and then transferred to a spectrometer through an 8-m long and 40 channels of bundled optical fiber array. The spectrograph covers the plasma radially from  $x = -20$  cm to  $x = 20$  cm. The observable wavelength of the spectrograph is in the range of  $2000 \text{ \AA}$  to  $5000 \text{ \AA}$ . The image of the exit plane of the spectrograph is focused onto an image intensifier tube (Hamamatsu V4435U) coupled with the CCD camera (Sony TK-66 for central cell system and XC-75 for anchor cell system). The frame rate of the CCD camera is 30 frame/s and the shutter speed is 10 ms. The two UV/V spectrograph systems are absolutely calibrated by using a tungsten ribbon filament standard lamp.

The VUV spectrograph (Fig. 2) can provide spatial and spectral distributions of plasma radiation in the wavelength range  $150\text{--}1050 \text{ \AA}$ . It consists of an entrance slit of limited height ( $100 \mu\text{m} \times 6 \text{ mm}$ ), an aberration-corrected concave grating with varied spacing grooves (Hitachi P/N001-0464), and an image-intensified two-dimensional detector system. One can observe the upper half of the plasma with a field of view of about 25-cm diameter. The SX spectrograph system (Fig. 3) is the same as the VUV spectrograph in the optical system of spatial imaging. The grating (Hitachi P/N 001-0266) is designed to cover the  $20\text{--}350 \text{ \AA}$  wavelength range. This spectrograph also settled on the GAMMA 10 so as to observe the upper half of a plasma about 20 cm in radial direction. The detector systems of both the VUV and the SX spectrograph consist of microchannel-plates (MCP) intensified image detector assemblies (Hamamatsu F2814-23P,  $50 \times 50 \text{ mm}^2$ ) and image recording cameras (Reticon MC9256) with fast scanning controllers (CCD RS9100). The frame rate of the cameras with full image

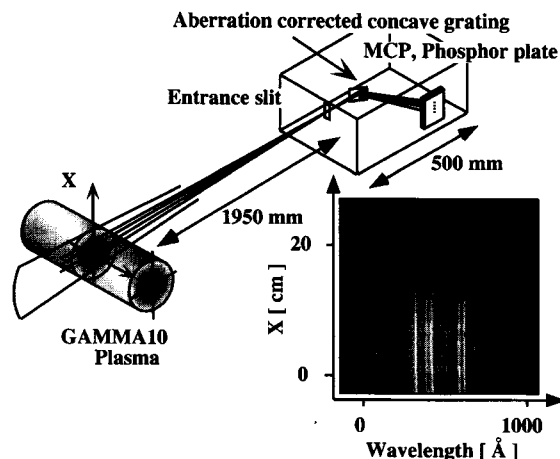


Fig. 2 Schematic of VUV spectrograph.

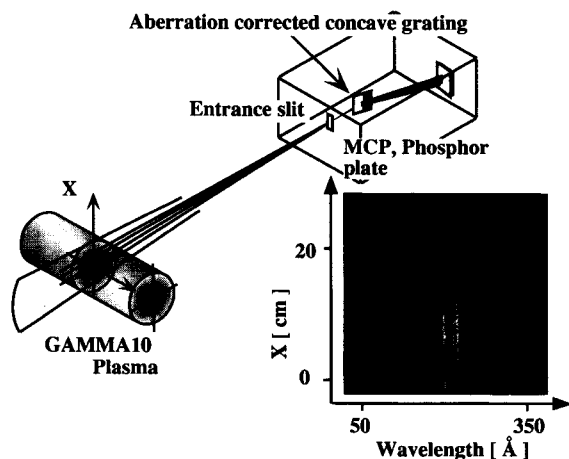


Fig. 3 Schematic of SX spectrograph.

size,  $256 \times 256$  pixels, can be varied from 4 to 106 frame/s. Absolute calibration experiments for these spectrographs have been performed on the overall sensitivities for the covered wavelength by using synchrotron radiation at the Photon Factory in the High Energy Accelerator Research Organization [6,9].

### 3. Spectroscopic Measurements in the GAMMA 10

The GAMMA 10 is a 27m long tandem mirror consisting of a 5.6 m long axisymmetric central cell, two anchor cells for suppressing MHD instability and axisymmetric end mirrors for forming plug/barrier potentials. Plasmas in the central cell are produced and heated by ICRH with hydrogen gas puffing and the plug potentials are produced by ECRH. The typical plasma

parameters in the central cell are as follows; the electron density is  $2 \times 10^{12} \text{ cm}^{-3}$ , the electron temperature is 80 eV and the ion temperature is 5 keV. The maximum plasma duration is 0.5 sec and the maximum duration of potential formation is reached to 0.15 sec. The two UV/V spectrographs are settled on the central cell and the anchor cell. The VUV and the SX spectrographs are set on the central cell and the barrier cell, respectively.

Some examples of measured spectra by using these spectrographs are shown in Fig. 4. Figures 4 (a) and (b) show the spectra of OV (278–279 nm) lines measured by the UV/V spectrographs in the central cell and the anchor cell, respectively. Figures 4 (c) and (d) show the VUV spectrum in the central cell and the SX spectrum in the barrier cell, respectively.

In the GAMMA 10 central cell region the absolute emission intensities were measured along radial direction by the UV/V and VUV spectrographs. The total emission intensity of various ions line spectrum and continuum spectrum throughout the UV/V and VUV regions were integrated over plasma cross section and plasma volume. The total power of emitted spectrum obtained from the above procedure was determined to be less than 1 kW, which can be thought as the radiation loss in the central cell. This power corresponds to be 0.5% of the total heating power of the GAMMA 10. Therefore the radiation loss is not a severe problem in the GAMMA 10.

The Doppler broadening measurements by using the UV/V spectrographs showed that the OV ion temperature was about 0.4 keV in the central cell and 7 keV in the anchor cell (Fig. 4 (a) and (b)). This significant difference in the OV ion temperature is thought to come from the following reason. The cyclotron frequency of  $O^{4+}$  ion in the anchor cell is equal to  $\omega_{ci}/4$ , where  $\omega_{ci}$  corresponds to the fundamental cyclotron frequency of hydrogen ions. The frequency of fundamental ICRH waves is equal to  $\omega_{ci}$  in the anchor cell. The  $O^{4+}$  ions could be heated due to cyclotron higher harmonic heating [1].

Radial profiles of the electrostatic potential also obtained by using the UV/V spectrograph [2,3]. Figure 5 shows the typical results of electrostatic potentials obtained by using plasma rotation measurements in the  $E \times B$  rotation dominant plasma, Fig. 5 (a) shows the electron density, Fig. 5 (b) and (c) show the impurity density and the electrostatic potential profiles, respectively. The potential difference between the center and the edge is 0.9 kV. The beam probe measurement provided the 1–1.2 kV of potential difference in the

similar plasma. Therefore these measurements are consistent each other.

We compared the CII line (904 Å) intensity measured by the VUV spectrograph to that from CR-

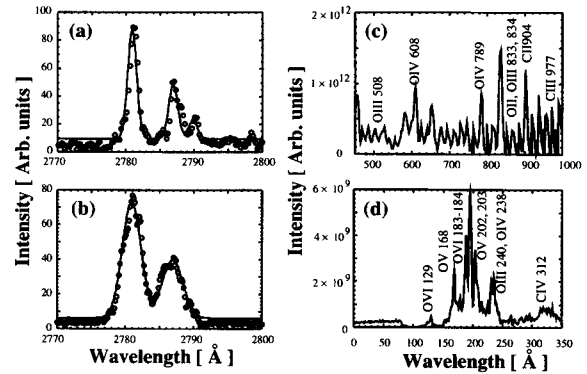


Fig. 4 (a) and (b) show the spectrum of OV lines measured by UV/V spectrograph in the central cell and the anchor cell, respectively. (c) shows VUV spectrum in the central cell and (d) shows the SX spectrum in the barrier cell.

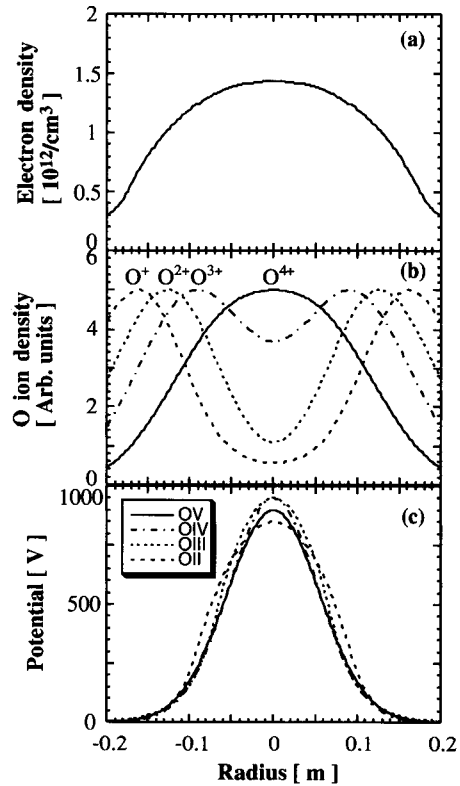


Fig. 5 (a) shows the electron density, (b) and (c) show the impurity density and the electrostatic potential profiles, respectively.

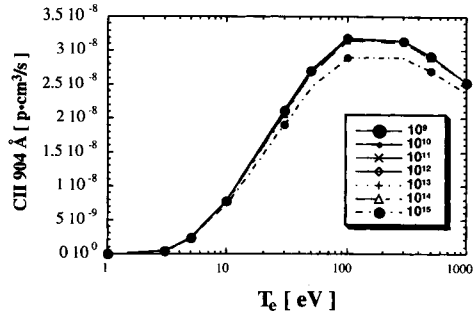


Fig. 6 CRM calculation results about CII line (904 Å) intensity.

model calculation in order to obtain the total  $C^+$  ion density. Figure 6 shows the calculated emissivity of CII line (904 Å). The CII line absolute emissivity was obtained by a procedure described before [6]. The plasma density and the electron temperature were measured by microwave interferometer and SX measurement, respectively. Then we can calculate the  $C^+$  ion density using CR-model calculation. The  $C^+$  ion density of the plasma center is about  $2 \times 10^7 \text{ cm}^{-3}$ . It is comparable to the result obtained by the same procedure of calculation of CII line (4267 Å) measured by the UV/V spectrograph.

Time dependent C ion radial profiles in the 0.2-sec long plasma measured by the VUV spectrograph are shown in Fig. 7. From the results of this C ion behavior, we could make a scenario of impurity transport in the GAMMA 10 tandem mirror. First, the impurities are sputtered from the vacuum vessel wall by the electron impact and the charge exchange neutral particle impact and enter into the plasma during the plasma production and buildup phases. Next, the impurities are ionized by the electron impact and the ion impact. As the plasma grows, the charged states of impurity ions are progressing, and the peak position of impurity ions of each ionized state moves towards the outer region. When the ECRH power is injected into the plug/barrier region, the plug potential is maintained. Then, the ions, hydrogen ions and impurity ions, are axially confined by the plug potential. After ECRH ceases, the impurity ion peaks appear in the same region as that before ECRH is on.

#### 4. Conclusion

We constructed the absolutely calibrated spectroscopic measurement systems in the wavelength range from SX to visible lights. We observed the

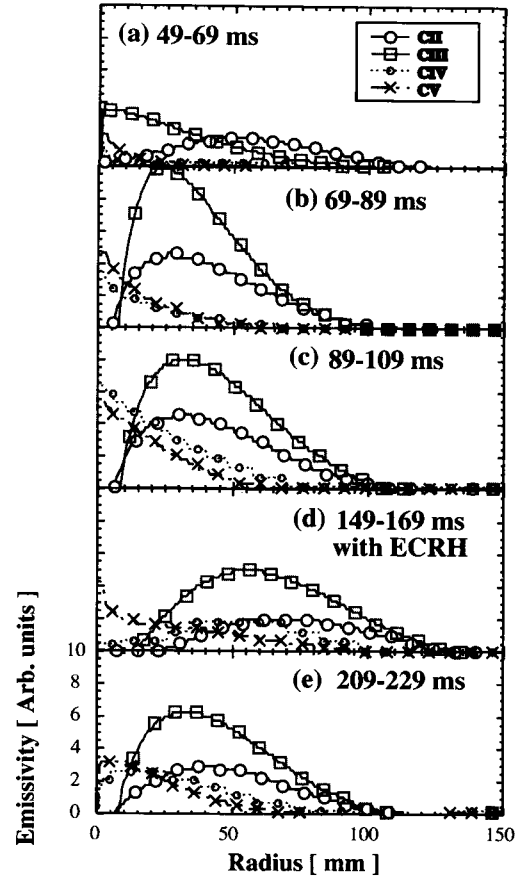


Fig. 7 Time dependent C ion radial profiles in the 0.2-sec long plasma measured by VUV spectrograph.

impurity line intensities, Doppler line broadenings, Doppler shifts by UV/V spectrograph and time dependent radial profiles of the impurity lines by the VUV and the SX spectrographs in the GAMMA 10. We obtained radiation loss in the wavelength range from visible to VUV in the GAMMA 10 central cell. Moreover we obtained  $C^+$  ion density in the central cell. These spectroscopic systems could be powerful tools to diagnose the GAMMA 10 plasma in a long pulse operation.

#### Acknowledgments

We would like to thank the GAMMA 10 group for their operational and diagnostic support and for useful discussions. This work was supported by a grant-in-aid for Scientific Research from the Ministry of Education, Science, Sports and Culture, Japan. Part of this work was performed under the approval of the Photon Factory Advisory Committee.

**References**

- [1] K. Ikeda *et al.*, *Rev. Sci. Instr.* **70**, 332 (1999).
- [2] K. Ikeda *et al.*, *Phys. Rev. Lett.* **78**, 3872 (1997).
- [3] K. Ikeda *et al.*, *Nucl. Fusion*. **38**, 1531 (1998).
- [4] N. Yamaguchi *et al.*, *Rev. Sci. Instrum.* **65**, 3408 (1994).
- [5] M. Yoshikawa *et al.*, *Jpn. J. Appl. Phys.* **38**, 2137 (1999).
- [6] M. Yoshikawa *et al.*, *PF Activity Rep.* **15**, 126 (1998).
- [7] M. Yoshikawa *et al.*, *J. Synchrotron Rad.* **5**, 762 (1998).
- [8] N. Yamaguchi *et al.*, *J. Plasma Fusion Res.* **71**, 867 (1995).
- [9] M. Yoshikawa *et al.*, *PF Activity Rep.* **16**, 291 (1999).
- [10] T. Kato *et al.*, *Fusion Eng. Des.* **34-35**, 789 (1997).